Biosensors and Bioelectronics 77 (2016) 56–61

Contents lists available at ScienceDirect

Biosensors and Bioelectronics

journal homepage: www.elsevier.com/locate/bios

Real-time monitoring of 3D cell culture using a 3D capacitance biosensor

Sun-Mi Lee [a,1], Nalae Han [b,1], Rimi Lee [c], In-Hong Choi [d], Yong-Beom Park [e], Jeon-Soo Shin [f,*], Kyung-Hwa Yoo [a,b,**]

[a] Nanomedical Graduate Program, Yonsei University, Seoul 120-749, Republic of Korea
[b] Department of Physics, Yonsei University, Seoul 120-749, Republic of Korea
[c] Center for Nano-Bio Measurement, Korea Research Institute of Standards and Science (KRISS), Daejeon 305-340, Republic of Korea
[d] Department of Microbiology, BK21 PLUS Project for Medical Science, Yonsei University College of Medicine, Seoul 120-752, Republic of Korea
[e] Division of Rheumatology, Department of Internal Medicine, Institute for Immunology and Immunological Disease, BK21 PLUS Project for Medical Science, Yonsei University College of Medicine, Seoul 120-749, Republic of Korea
[f] Department of Microbiology, BK21 PLUS Project for Medical Science, Severance Biomedical Science Institute and Institute for Immunology and Immunological Disease, Yonsei University College of Medicine, Seoul 120-752, Republic of Korea

ARTICLE INFO

Article history:
Received 14 July 2015
Received in revised form
2 September 2015
Accepted 3 September 2015
Available online 6 September 2015

Keywords:
Three-dimensional (3D) cell culture
Capacitance sensor
Real-time monitoring
Proliferation
Apoptosis
Migration

ABSTRACT

Three-dimensional (3D) cell cultures have recently received attention because they represent a more physiologically relevant environment compared to conventional two-dimensional (2D) cell cultures. However, 2D-based imaging techniques or cell sensors are insufficient for real-time monitoring of cellular behavior in 3D cell culture. Here, we report investigations conducted with a 3D capacitance cell sensor consisting of vertically aligned pairs of electrodes. When GFP-expressing human breast cancer cells (GFP-MCF-7) encapsulated in alginate hydrogel were cultured in a 3D cell culture system, cellular activities, such as cell proliferation and apoptosis at different heights, could be monitored non-invasively and in real-time by measuring the change in capacitance with the 3D capacitance sensor. Moreover, we were able to monitor cell migration of human mesenchymal stem cells (hMSCs) with our 3D capacitance sensor.

1. Introduction

Traditional two-dimensional (2D) monolayer cell cultures have been widely used for various studies ranging from cancer drug screening to developmental biology; however, recent work has shown that cells often exhibit unnatural behavior when excised from native three-dimensional (3D) tissues and confined to a monolayer (Mulhall et al., 2013; Tibbitt and Anseth, 2009). Hence, 3D cell cultures have been introduced and extensively studied (Mueller-Klieser, 1997; Abbott, 2003). In 3D cell culture, cells are encapsulated within 3D scaffolds; this 3D culture system provides a more physiologically relevant microenvironment, allowing cells to form natural shapes and intercellular contacts (Liu et al., 2012; Tibbitt and Anseth, 2009).

When cells are cultured in 2D substrates such as polystyrene and glass, their number and morphology are usually examined using an optical microscope. To further study cellular activities, optical methods based on fluorescent probes are commonly adopted. However, fluorescent staining normally kills cultured cells; consequently, optical methods combined with fluorescent dye staining provide little information about the kinetics of cellular responses. As an alternative approach for real-time, non-invasive, and label-free measurements, electric cell-substrate impedance sensors (ECIS) have been developed (Giaever et al., 1984; Daza et al., 2013; Jeong et al., 2012; Nguyen et al., 2013). In ECIS, the alternating current (ac) impedance between a small sensing electrode and a large counter-electrode is measured, while cells are cultured on a gold (Au) sensing electrode. Because cells are very poor conductors at low frequencies (< 10 kHz), the electrode impedance increases if cells attach and proliferate on the surface of the working electrode. Conversely, if cells are dead, they are

* Corresponding author at: Department of Microbiology, BK21 PLUS Project for Medical Science, Severance Biomedical Science Institute and Institute for Immunology and Immunological Disease, Yonsei University College of Medicine, Seoul 120-752, Republic of Korea.
** Corresponding author at: Department of Physics, Yonsei University, Seoul 120-749, Republic of Korea.
E-mail addresses: jsshin6203@yuhs.ac (J.-S. Shin), khyoo@yonsei.ac.kr (K.-H. Yoo).
[1] Equal contribution to the manuscript.

http://dx.doi.org/10.1016/j.bios.2015.09.005
0956-5663/

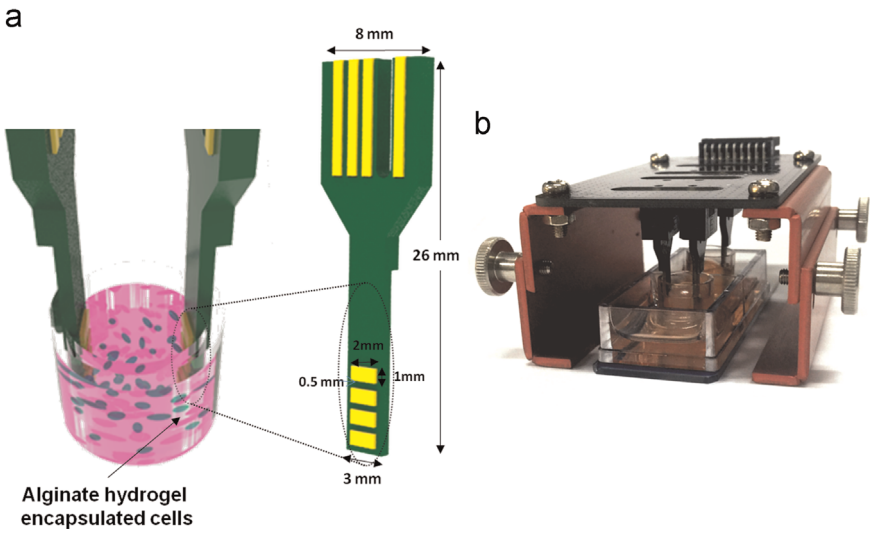

Fig. 1. Schematics (a) and images (b) of a 3D capacitance sensor consisting of four pairs of vertically aligned electrodes.

released from the surface of the sensing electrode, causing a decrease in electrode impedance. In 3D cell culture, however, cells are encapsulated in a 3D matrix and thus cannot attach to the sensing electrode surface. Moreover, it is difficult to observe and quantify encapsulated cells microscopically without slicing the 3D matrix. Therefore, the above approaches may not be applicable in 3D cell cultures.

Here, we report a 3D capacitance sensor that consists of four pairs of vertically aligned electrodes to monitor cellular activities in real-time in 3D cell cultures (Fig. 1(a)). In our previous work, we reported that various cellular activities, such as proliferation, apoptosis/necrosis (Lee et al., 2009), endocytosis (Lee et al., 2010), and differentiation (Lee et al., 2015), could be monitored in real-time by measuring the change in capacitance or dielectric constant when cells are cultured on 2D substrates. In a 2D capacitance sensor, cells are placed between the two electrodes rather than on the sensing electrode, unlike in ECIS; therefore, it is expected that cellular activities may be monitored in real-time by measuring the capacitance change with vertically aligned pairs of electrodes, even in 3D cell culture. Indeed, vertical information about cellular behaviors can be obtained non-invasively with our 3D capacitance sensor when cells encapsulated in non-toxic and biocompatible alginate hydrogel are cultured in a 3D culture system (Kaklamani et al., 2014).

2. Materials and methods

2.1. Cell cultures

GFP-expressing human breast cancer cells (GFP-MCF-7; ATCC, Manassas, VA, USA) were cultured in Modified Eagle's Medium (MEM; Gibco, Rockville, MD, USA) containing 10% fetal bovine serum (PAA Laboratories, Somerset, UK), 1% penicillin–streptomycin, 1% fungizone (Gibco), 22.5 μM HEPES, and 2 μM L-glutamine. Human mesenchymal stem cells (hMSCs) were obtained from the Cell Therapy Center at Yonsei University (YUHS; Seoul, Korea) and cultured in MEM containing MEM-F12 supplemented with 2% B27 (Life Technologies, Grand Island, NY, USA), EGF (20 ng/mL; R&D Systems, Minneapolis, MN USA), and FGF-2 (20 ng/mL; R&D Systems,). All cell cultures were conducted inside a humidified incubator maintained at 37 °C and 5% CO_2.

2.2. Alginate hydrogel scaffold

Alginate sodium salt from brown algae (low viscosity; Sigma, St. Louis, MO, USA) was dissolved in MEM culture medium to a 3% concentration (w/w). For cell encapsulation, GFP-MCF-7 or hMSCs were homogeneously suspended in 3% sodium alginate solution. Cells in sodium alginate solution (0.8 mL) were then transferred to Millicell® cell culture inserts (diameter: 12 mm, pore size: 12 μm; Millipore, Billerica, MD USA). To crosslink the alginate hydrogel, the Millicell® inserts containing the alginate solution and cells were immersed in 100 mM $CaCl_2$-buffered MEM culture medium and left for 2 h in a 37 °C humidified incubator with 5% CO_2, resulting in formation of a hydrogel scaffold (Fig. S1). Subsequently, the alginate hydrogel-encapsulated cells were cultured in MEM culture medium (2 mL) inside the incubator; the medium was changed every 2 days.

Specimens consisting of four layers with different cell densities of GFP-MCF-7 were prepared as follows. First, a mixture of sodium alginate solution (0.2 mL) and GFP-MCF-7 cells (10^2 cells/mL) was poured into Millicell® inserts and gelated by immersing in 100 mM $CaCl_2$-buffered MEM culture medium and leaving for 0.5 h in a 37 °C humidified incubator with 5% CO_2, leading to formation of a hydrogel scaffold containing 10^2 cells/mL of GFP-MCF-7. Next, similar processes were repeated three more times with different cell densities, resulting in three more hydrogel scaffolds with different cell densities. Finally, four hydrogel scaffolds containing different cell densities of GFP-MCF-7 (10^2, 10^3, 10^4, and 10^5 cells/mL) were vertically stacked inside the Millicell® inserts. Specimens with different cell densities of hMSCs were prepared similarly.

2.3. Fabrication of a 3D capacitance sensor

A capacitance-based cell sensor consisting of four pairs of electrodes was constructed by attaching two printed circuit boards (PCBs), as shown in Fig. S2. First, four parallel electrodes (1×2 mm^2) with 0.5-mm spacing and four electrical connections to external connectors were patterned on a double-sided PCB and gold-plated (Fig. S2(a)). On a single-sided PCB, four electrodes, electrical connections, and connection lines between electrodes and electrical connections were patterned and gold-plated (Fig. S2 (b)). Next, two PCBs were attached to embed connection lines, exposing only four electrodes to cells encapsulated in the alginate

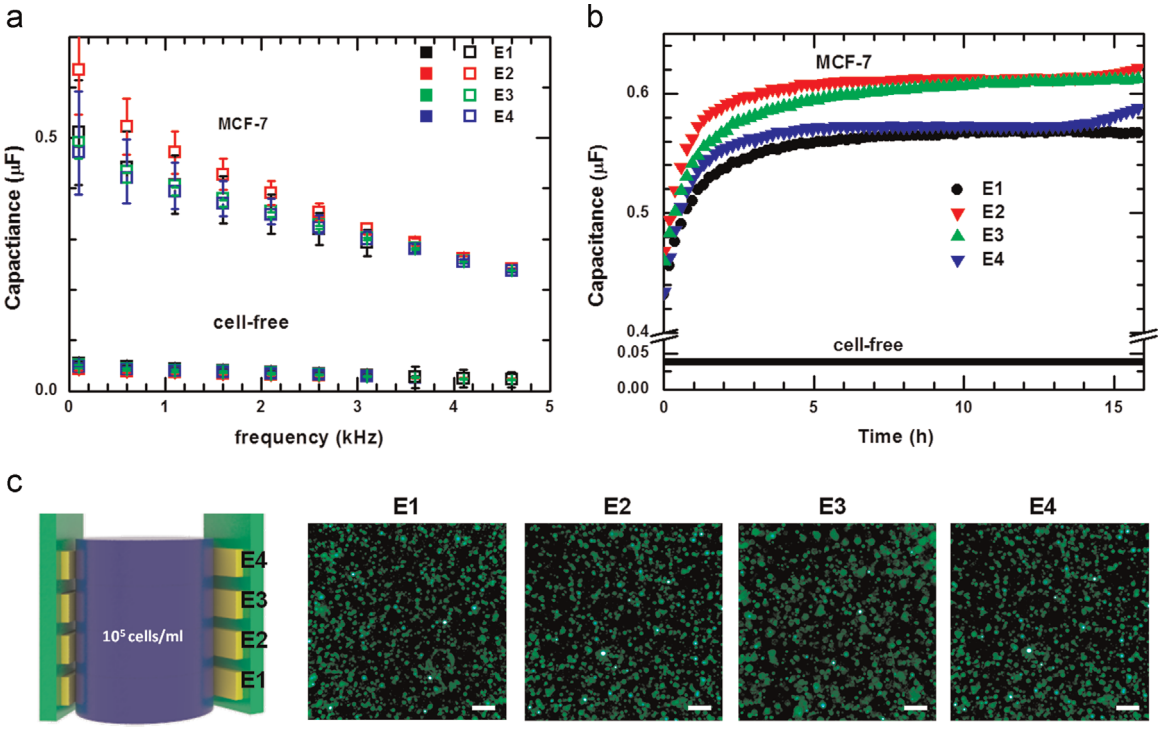

Fig. 2. (a) Frequency dependence of capacitance measured with electrodes 1–4 (E1–E4) in cell-free and GFP-MCF-7 cell-encapsulated hydrogels. Data represent mean ± standard deviation ($n=3$). (b) Real-time capacitance measured with E1–E4 in cell-free and GFP-MCF-7 cell-encapsulated hydrogels. (c) Fluorescent optical images of a GFP-MCF-7 cell-encapsulated hydrogel horizontally sliced after 16 h of culture (scale bar: 100 μm).

hydrogel (Fig. S2(c)). To place the capacitance cell sensor vertically inside the Millicell® inserts, a supporting stand was constructed with aluminum plates (Fig. 1(b)).

2.4. Capacitance measurements

Capacitance was measured by an LCR meter (Agilent 4294A, CA, USA) with a peak-to-peak ac signal of 10 mV at frequencies ranging from 100 Hz to 5 kHz. The sensor inside the incubator and LCR meter outside the incubator were connected via electrical connectors mounted on the side of the incubator. Capacitance was measured simultaneously from two sensors with a data acquisition/switching unit (Agilent 34970A) connected to the LCR meter. Data were collected every 10 min from each sensor.

2.5. Staining of nuclear DNA

Sections of 1-mm thickness were obtained from alginate hydrogel-encapsulated hMSCs by using a razor blade after 48 h of incubation. Sections were washed twice with PBS and immersed in 10 μg/mL Hoechst 33342 (20 mM; Sigma, St. Louis, MO, USA) for 30 min at 37 °C, followed by examination with a fluorescence microscope.

3. Results and discussion

3.1. Real-time measurement of cell viability

To investigate whether cell viability could be monitored in real-time in a 3D culture system, a 3D capacitance sensor consisting of four parallel electrodes was placed vertically inside a Millicell® insert (Fig. 1(b)). GFP-MCF-7 cells (1×10^5 cells/mL) in 3 wt% alginate solution were then added into the Millicell® insert (Fig. S1), and the Millicell® insert was immersed in buffered $CaCl_2$ (100 nM) at 37 °C for 3 h to crosslink the alginate hydrogel. For cell culture, $CaCl_2$-buffered media were replaced with cell culture media and

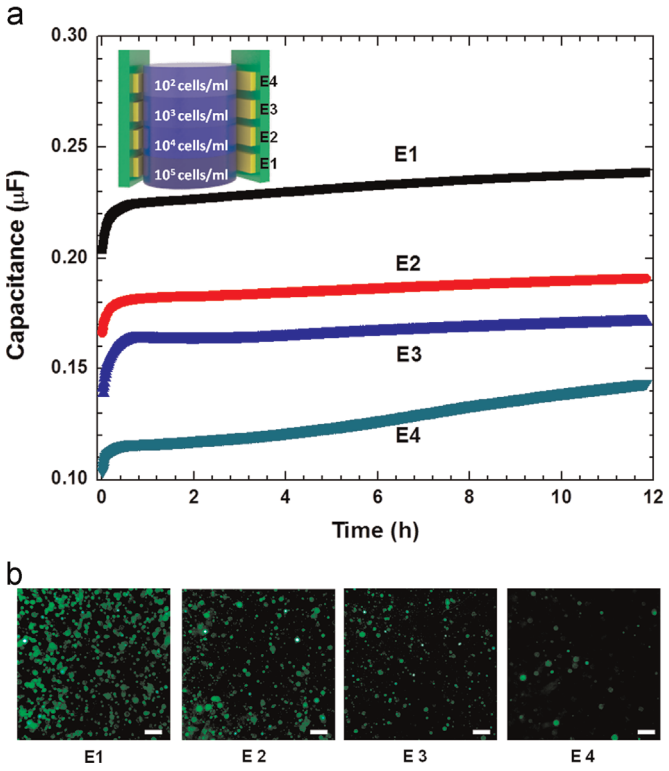

Fig. 3. (a) Real-time capacitance measured with electrodes 1–4 (E1–E4) in hydrogels containing different GFP-MCF-7 cell densities. (b) Fluorescent optical images of hydrogels containing different GFP-MCF-7 cell densities. Hydrogels were horizontally sliced after 12 h of culture for fluorescence imaging (scale bar: 100 μm).

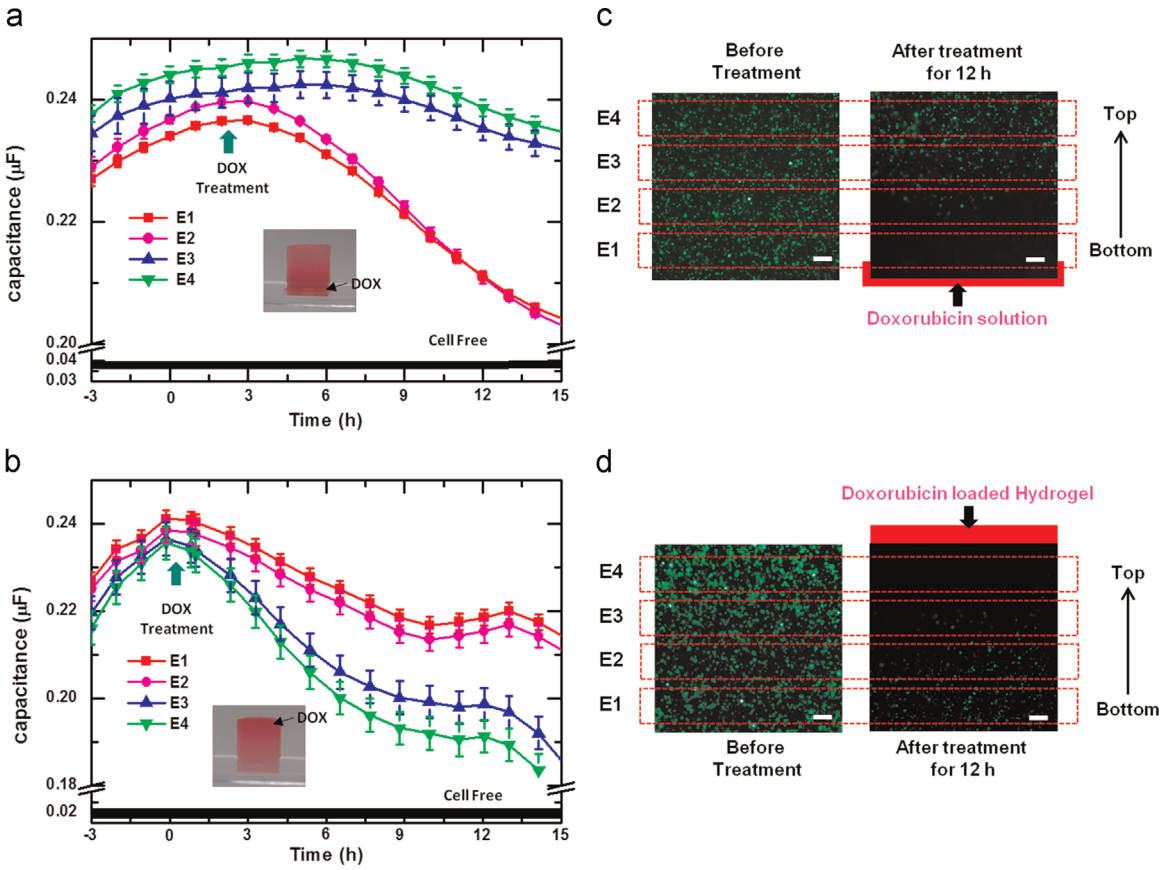

Fig. 4. Real-time capacitance measured with electrodes 1–4 (E1–E4) for a GFP-MCF-7 cell- encapsulated hydrogel treated with DOX from the bottom (a) and the top (b). Fluorescent optical images of a GFP-MCF-7 cell-encapsulated hydrogel vertically sliced after 12 h of treatment with DOX from the bottom (c) and the top (d) (scale bar: 100 μm). Data represent mean ± standard deviation ($n=3$). Error bars are depicted for every fifth data point for visual clarity.

placed inside a humidified incubator. Fig. 2(a) shows the frequency dependence of capacitance measured using four pairs of electrodes (E1–E4) just after placing the Millicell® insert inside the incubator for both GFP-MCF-7 cell-encapsulated and cell-free (control) hydrogels. For both specimens, the capacitance decreased with increasing frequency. However, the capacitance of GFP-MCF-7 cell-encapsulated hydrogels was higher than that of the cell-free hydrogel because the dielectric constant increased with the cell volume (Lee et al., 2015). To determine whether capacitance was dependent on the concentration of alginate solution, the frequency dependence of capacitance was measured for the cell-free hydrogel at concentrations of 1, 3, and 5 wt% alginate (Fig. S3). The capacitance values were unaffected by hydrogel concentration.

Fig. 2(b) shows the time dependence of capacitance measured at a frequency of 1 kHz for GFP-MCF-7 cell-encapsulated and cell-free hydrogels, during GFP-MCF-7 cell culture. The capacitance of GFP-MCF-7 cell-encapsulated hydrogels increased with time, whereas that of cell-free hydrogels was nearly unchanged, implying that the increase in capacitance was due to proliferation of GFP-MCF-7 cells. Fluorescent images of a GFP-MCF-7 cell-encapsulated hydrogel horizontally sliced after 16 h of culture are shown in Fig. 2(c). The fluorescence intensity was almost uniform horizontally and vertically, indicating that cells thrived in the alginate hydrogel-containing Millicell® insert. Lei et al. (2014) reported similar electrical measurements with vertical electrodes in a 3D cell culture microfluidic chip to monitor cellular activity. They observed an increase in impedance during proliferation because cells are poor conductors at low frequencies. However, they used a single pair of electrodes; thus, they could not differentiate among cellular activities at different heights.

Next, we prepared alginate hydrogels containing different densities of GFP-MCF-7 cells (10^2, 10^3, 10^4, and 10^5 cells/mL) to investigate the dependence of capacitance on cell density. These hydrogels were vertically stacked (inset of Fig. 3(a)), and real-time capacitance was measured with E1–E4 (Fig. 3(a)). Higher values of capacitance were measured for higher cell densities, although the rate of capacitance increase was higher at lower cell densities, which was probably due to the greater free space available at lower cell densities (Fig. 3(b)). These observations indicate that capacitance increased as the density of living cells increased.

3.2. Real-time measurement of cell apoptosis for drug response

In addition to monitoring cell viability, we investigated whether chemosensitivity could be non-invasively monitored in real-time with our 3D capacitance sensor. To induce apoptosis, the anticancer drug doxorubicin (DOX) was added to the culture media (inset of Fig. 4(a)) or a DOX-loaded hydrogel was placed on top of GFP-MCF-7 cells encapsulated in the alginate hydrogel (inset of Fig. 4(b)). Capacitance was then measured by E1–E4 as a function of time. When DOX (200 μL, 100 ng/mL) was added to the culture media, it diffused upward (Fig. S4(a)). Thus, the capacitance measured by the bottom electrodes, E1 and E2, decreased more rapidly than the capacitance measured by the top electrodes, E3 and E4 (Fig. 4(a)). In contrast, when a DOX-loaded hydrogel (200 μL, 100 ng/mL) was placed on top of the GFP-MCF-7 cell-encapsulated hydrogel, DOX diffused downward (Fig. S4(b)). Consequently, a more rapid decrease in capacitance was observed

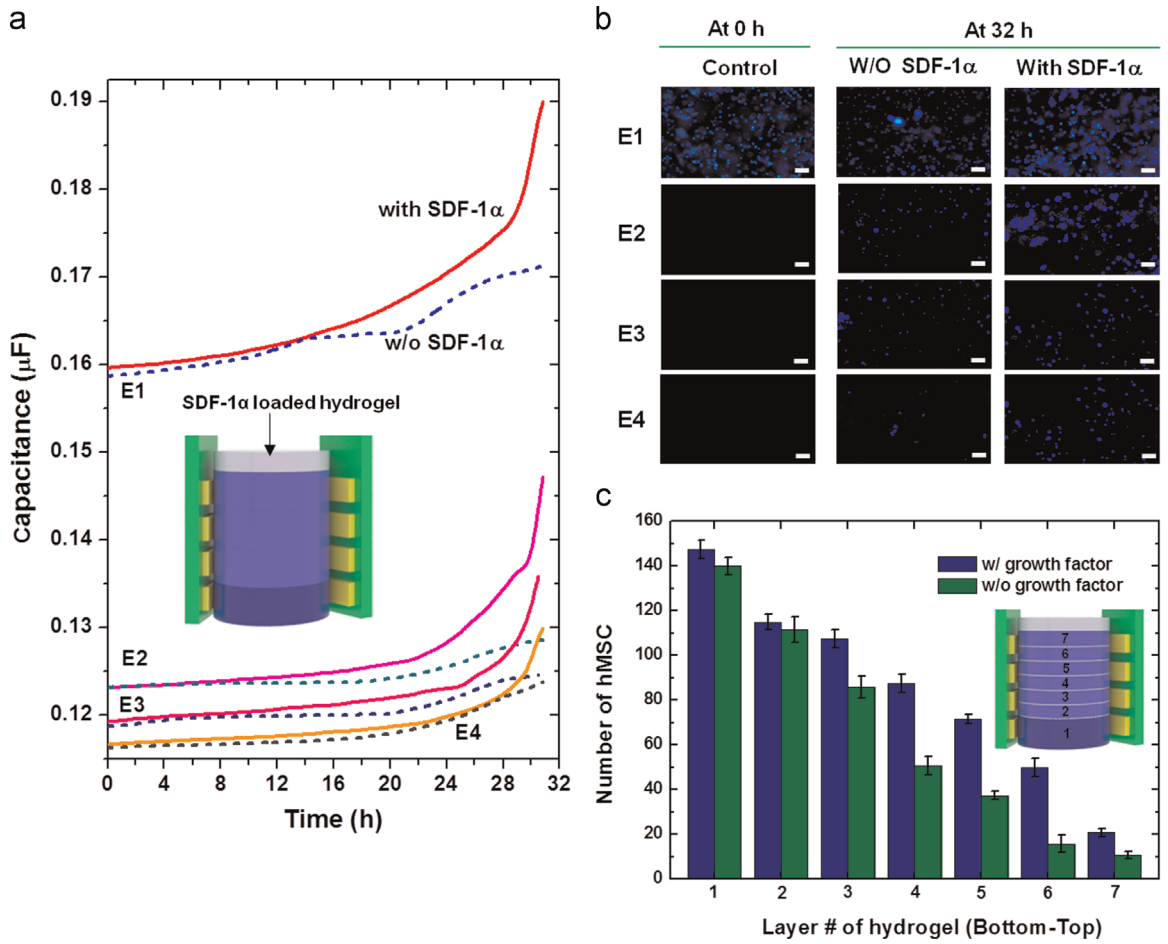

Fig. 5. (a) Real-time capacitance measured with electrodes 1–4 (E1–E4) in hMSC-encapsulated hydrogels cultured with or without SDF-1. Error Bars are not shown for visual clarity. The data with error bars are shown in Fig. S5. (b) Fluorescent optical images of a hMSC-encapsulated hydrogel horizontally sliced and stained with DAPI before (left column) and after 32 h of culture without (middle column) or with SDF-1α (right column) (scale bar: 200 μm). (c) Numbers of hMSCs in seven layers of the hydrogel. Cell numbers were counted from fluorescent optical images of hMSC-encapsulated hydrogels horizontally sliced and stained with DAPI after 48 h of culture with or without SDF-1α.

by E3 and E4 than by E1 and E2 (Fig. 4(b)). These results suggest that cell death caused a decrease in capacitance, as reported in 2D cell culture (Lee et al., 2009).

Fluorescent images of vertically sliced GFP-MCF-7 cells encapsulated in an alginate hydrogel treated for 12 h with DOX from below and above are shown in Fig. 4(c) and (d), respectively. When DOX was added to the culture media, no florescence was detected at the bottom, whereas green fluorescence was observed at the top (Fig. 4(c)). These findings indicate that most GFP-MCF-7 cells in the bottom of the hydrogel were dead because of the high concentration of DOX, whereas most cells in the top region were alive because of the low concentration of DOX. However, when a DOX-loaded hydrogel was placed on top of the GFP-MCF-7 cell-encapsulated alginate hydrogel, the opposite was observed (Fig. 4 (d)): no florescence was detected at the top, whereas green fluorescence was observed at the bottom of the hydrogel. These results demonstrate that cytotoxicity can be monitored in real-time with our 3D capacitance sensor.

3.3. *Real-time measurement of cell migration*

Finally, to investigate whether cell migration can be monitored with our 3D capacitance sensor, we prepared a 3 wt% alginate hydrogel containing 5×10^4 cell/mL hMSCs only in the bottom layer and few cells in the top layer (inset of Fig. 5(a)). Real-time capacitance was then measured by E1–E4 while cells were cultured with or without the recombinant human stromal cell-derived factor-1 alpha/CXCL12 (SDF-1α; Prospec-Tany TechnoGene Ltd., Ness-Ziona, Israel). SDF-1α (200 μL, 100 ng/mL) was loaded inside the hydrogel and placed on top of the hMSC-encapsulated alginate hydrogel for slow release (inset of Fig. 5(a)). SDF-1α binds to the CXCR4 receptor and modulates MSC migration and cytokine secretion (Dar et al., 2005; Liu et al., 2011). Initially, the capacitance of the bottom layer, measured using E1, was higher than the capacitance of the upper layers, measured using E2, E3, or E4, because most cells were present in the bottom layer. For hMSCs cultured in the absence of SDF-1α, the capacitance of the upper layers was nearly unchanged until 20 h after loading, and then increased slowly because of a low rate of spontaneous migration of hMSCs (Ponte et al., 2007). However, in the presence of SDF-1α, the capacitance of the upper layers increased rapidly from approximately 24 h after loading (Figs. 5(a) and S5). In addition, the capacitance of the bottom layer increased more rapidly in the presence than in the absence of SDF-1α. Because SDF-1α is known to accelerate proliferation and migration (Wynn et al., 2004; Ji et al., 2004), these results imply that information about vertical cell migration can be obtained in real-time with our 3D capacitance sensor.

Fig. 5(b) shows fluorescent optical images of a hMSC-encapsulated hydrogel that has been horizontally sliced and the nuclei have been stained after 32 h of culture with or without SDF-1α. Before culture, no cells were observed in the upper layers.

After 32 h of culture, however, live cells were observed in the upper layers, indicating that cells had migrated upward. Moreover, in the presence of SDF-1α, higher cell densities were noted in all layers (Figs. 5(c) and S6), which we ascribed to an increase in cell proliferation and migration caused by SDF-1α. These findings are consistent with real-time capacitance data shown in Fig. 5(a) and demonstrate that cell migration can be monitored in real-time with our 3D capacitance sensor.

4. Conclusions

We fabricated a 3D capacitance sensor comprised of vertically aligned electrode pairs and used it to measure real-time capacitance when GFP-MFP-7 cells encapsulated in an alginate hydrogel were cultured in a 3D culture system. As the number or volume of live cells increased, the capacitance correspondingly increased. Therefore, vertical information on cell viability and chemosensitivity was obtained in real-time by measuring capacitance with electrodes at different heights. In addition, hMSC migration could be non-invasively monitored in real-time with the 3D capacitance sensor. Our 3D capacitance sensors can be easily integrated into array chips; thus, this dielectric method can be applied to high-throughput drug screening based on 3D cell cultures and to the monitoring of regenerative medicine.

Acknowledgment

This work has been financially supported by the Basic Science Research Program through the National Research Foundation of Korea (NRF) funded by the Ministry of Science, ICT and Future Planning (Grant nos. 2011-0017486, 2012R1A4A1029061, 2013R1A1A3A04009309, and 2011-0017611).

Appendix A. Supplementary material

Supplementary data associated with this article can be found in the online version at 10.1016/j.bios.2015.09.005.

References

Abbott, A., 2003. Nature 424, 870–872.
Dar, A., Goichberg, P., Shinder, V., Kalinkovich, A., Kollet, O., Netzer, N., Margalit, R., Zsak, M., Nagler, A., Hardan, I., Resnick, I., Rot, A., Lapidot, T., 2005. Nat. Immunol. 6, 1038–1046.
Daza, P., Olmo, A., Cañete, D., Yúfera, A., 2013. Sens. Actuator B – Chem. 176, 605–610.
Giaever, I., Keese, C.R., 1984. Proc. Natl. Acad. Sci. USA 81, 3761–3764.
Jeong, S.H., Lee, D.W., Kim, S., Kim, J., Ku, B., 2012. Biosens. Bioelectron. 35, 128–133.
Ji, J.F., He, B.P., Dheen, S.T., Tay, S.S., 2004. Stem Cells 22, 415–427.
Kaklamani, G., Cheneler, D., Grover, L.M., Adams, M.J., Bowen, J., 2014. J. Mech. Behav. Biomed. 36, 135–142.
Lee, R., Choi, H., Shin, J., Km, K., Yoo, K.H., 2009. Biosens. Bioelectron. 25, 1592–1596.
Lee, R., Kim, I.S., Han, N., Yun, S., Park, K.I., Yoo, K.H., 2015. Sci. Rep. 4, 1–7.
Lee, R., Kim, P.H., Choi, J.W., Kwon, O.J., Kim, K., Kim, D., Yun, C.O., Yoo, K.H., 2010. Biosens. Bioelectron. 25, 1325–1332.
Lei, F.K., Wu, M.H., Hsu, C.W., Chen, Y.D., 2014. Biosens. Bioelectron. 51, 16–21.
Liu, W., Thomopoulos, S., Xia, Y., 2012. Adv. Healthc. Mater. 1, 10–25.
Liu, X., Duan, B., Cheng, Z., Jia, X., Mao, L., Fu, H., Che, Y., Ou, L., Liu, L., Kong, D., 2011. Protein Cell 2, 845–854.
Mueller-Klieser, W., 1997. Am. J. Physiol. 273 (4 Pt. 1), C1109–C1123.
Mulhall, H.J., Hughes, M.P., Kazmi, B., Lewis, M.P., Labeed, F.H., 2013. Biochem. Biophys. Acta 1830, 5136–5141.
Nguyen, T.A., Yin, Y.I., Reyes, D., Urban, G.A., 2013. Anal. Chem. 85, 11068–11076.
Ponte, A.L., Marais, E., Gallay, N., Langonné, A., Delorme, B., Hérault, O., Charbord, P., Domenech, J., 2007. Stem Cells 25, 1737–1745.
Tibbitt, M.W., Anseth, K.S., 2009. Biotechnol. Bioeng. 103, 655–663.
Wynn, R.F., Hart, C.A., Corradi-Perini, C., O'Neill, L., Evans, C.A., Wraith, J.E., Fairbairn, L.J., Bellantuono, I., 2004. Blood 104, 1643–2645.